Molecular Therapy
Oncology
Original Article

Preclinical study of inetetamab combined with atezolizumab to synergistically inhibit HER2 and PD-L1 in the treatment of ovarian cancer

Feiquan Ying (应菲全),[1,4] Xuyang Zhou (周许阳),[1,2,4] Mengqing Chen (陈梦情),[1] Lin Huang (黄琳),[1] Lingling Gao (高玲玲),[1] Qing Zhao (赵青),[3] and Yuan Zhang (张媛)[1]

[1]Department of Obstetrics and Gynecology, Union Hospital, Tongji Medical College, Huazhong University of Science and Technology, Wuhan 430022, China; [2]Department of Medical Ultrasound, Yueyang Central Hospital, Yueyang 414000, China; [3]Department of Obstetrics and Gynecology, The Central Hospital of Wuhan, Tongji Medical College, Huazhong University of Science and Technology, Wuhan 430014, China

Epithelial ovarian cancer (EOC) is the deadliest gynecological malignancy. Precision treatments are crucial for improving patient survival. This research explored the potential anti-tumor effects of combining inetetamab and atezolizumab for HER2$^+$ EOC patients. The expressions of human epidermal growth factor receptor 2 (HER2) and programmed cell death ligand 1 (PD-L1) in EOC cells were evaluated. EOC cell-derived subcutaneous and peritoneal dissemination mouse models were used to evaluate the anti-tumor effects of inetetamab, with or without atezolizumab. The correlations between the expressions of HER2 and PD-L1 as well as the infiltration of T cells in tumors from patients and mice were analyzed by immunohistochemistry. Inetetamab suppressed the growth of HER2$^+$ tumors in mouse models. HER2 overexpression increased PD-L1 levels in EOC cells. The expression level of HER2 is positively related to that of PD-L1 in the tumors of EOC patients as well as the infiltration of both CD4$^+$ and CD8$^+$ T cells. The combination of inetetamab and atezolizumab impeded the growth of HER2$^+$ EOC tumors *in vivo* and induced a long-term anti-tumor effect with the elevated infiltration of CD103$^+$CD8$^+$ cells. These findings suggest that the combination of inetetamab and atezolizumab could be a promising precision treatment strategy for HER2$^+$ EOC patients.

INTRODUCTION

Epithelial ovarian cancer (EOC) is the most lethal malignant tumor in the female reproductive system, with an insidious onset and rapid progress.[1] Even though the therapy strategies of EOC have been optimized in recent decades, nearly 90% of patients suffer from cancer recurrence within 3 years after receiving the first-line therapy. The 5-year survival is still under 40%. Considering the heterogeneity of the genetic background in EOC, the precision treatment targeting different molecular characteristics of tumors is the key to improving the survival of EOC patients.[2,3]

Human epidermal growth factor receptor 2 (HER2) is a transmembrane tyrosine kinase receptor that was identified as an anti-tumor target in 1987. To date, anti-HER2 monoclonal antibodies (mAbs) have been the component of the first-line therapy for HER2$^+$ advanced breast cancer and HER2$^+$ advanced gastric cancer.[4,5] Even though the expression of HER2 is observed in some EOC patient tissues at a 10%–20% positive ratio, patients with positive HER2 expression have poor survival.[6,7] However, along with the failure of several clinical trials, including GOG 160, the therapeutic effect of HER2 mAb in EOC does not meet expectations.[8–10]

Anti-HER2 mAbs inhibit the progress of cancer via multiple mechanisms. In addition to blocking the signal transduction involving HER2, the antibodies are able to activate the antibody-dependent cell cytotoxicity (ADCC) and the antibody-dependent cell phagocytosis and induce the T cell-mediated memory of tumor-suppressive effects.[11] While these immune-related anti-tumor effects are highly dependent on the activated tumor immune microenvironment, most EOCs are "cold" tumors with an immunosuppressive microenvironment,[12] which may partly explain the unsatisfactory therapeutic effect of HER2 mAbs in EOC patients.

Immune checkpoint inhibitors are widely utilized in the therapy of cancers. mAbs targeting programmed cell death receptor 1 (PD-1) and its ligand, programmed cell death ligand 1 (PD-L1), present marked anti-tumor effects on lung cancer and malignant melanoma by relieving immunosuppression in tumors.[13] Nevertheless, immunotherapy has failed to show significant activity in other cancers, such as pancreatic cancer[14] and OC. The response rate of anti-PD-1/PD-L1

Received 18 July 2024; accepted 14 January 2025;
https://doi.org/10.1016/j.omton.2025.200938.

[4]These authors contributed equally

Correspondence: Qing Zhao, Department of Obstetrics and Gynecology, The Central Hospital of Wuhan, Tongji Medical College, Huazhong University of Science and Technology, Wuhan 430014, China.
E-mail: zhaoqing@zxhospital.com
Correspondence: Yuan Zhang, Department of Obstetrics and Gynecology, Union Hospital, Tongji Medical College, Huazhong University of Science and Technology, Wuhan 430022, China.
E-mail: yuanzhang75@hust.edu.cn

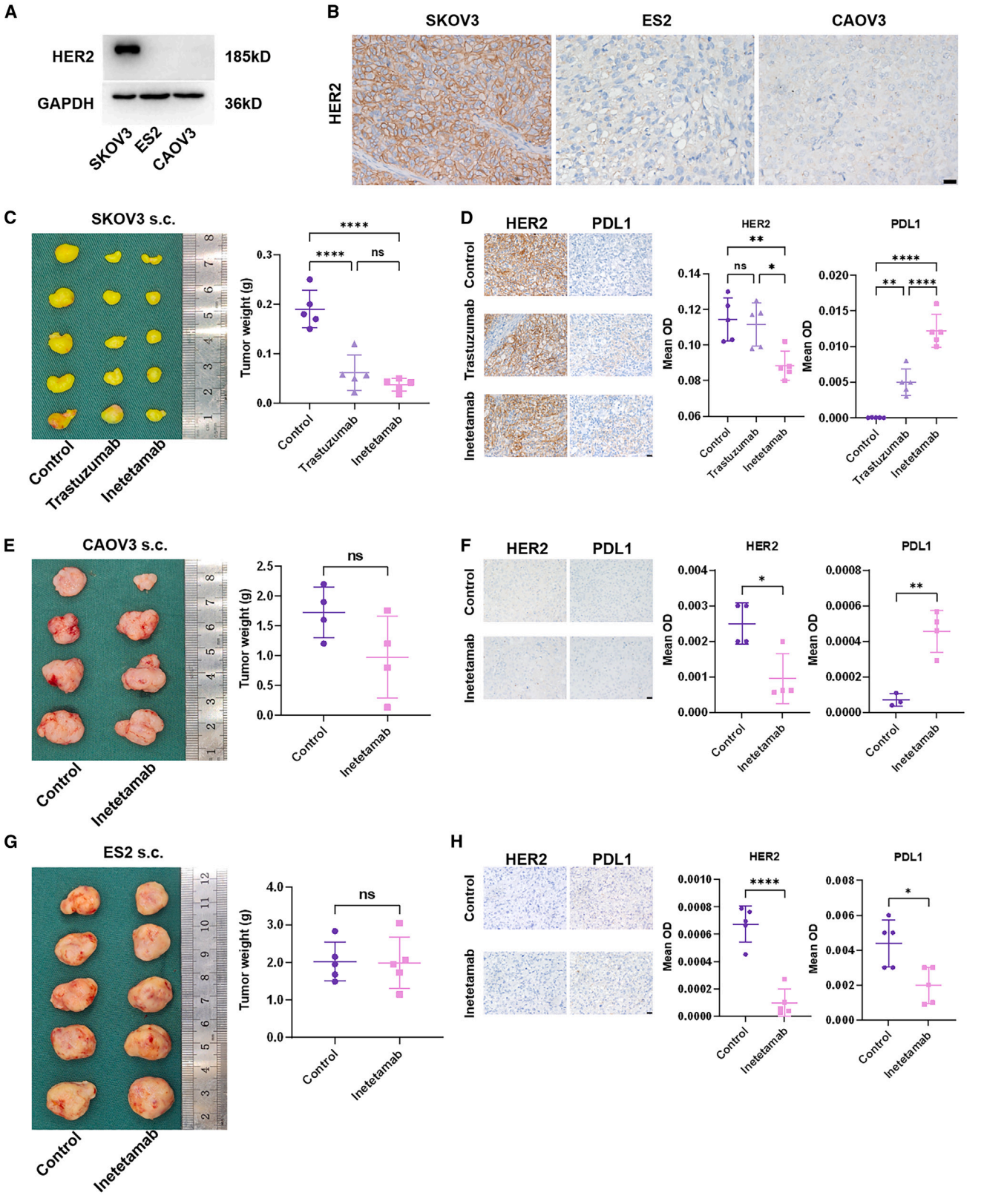

(legend on next page)

antibodies is less than 10% in recurrent OC patients.[15,16] A synergistic anti-tumor effect of anti-PD-1 therapy and trastuzumab was observed in HER2$^+$ gastric cancer.[17] In addition, the bispecific antibody targeting HER2 and PD-L1 is able to inhibit tumor growth with superior efficacy.[18] However, there are no reports on the combined use of anti-HER2 and anti-PD-1/PD-L1 mAbs in OC. Theoretically, the effect of the anti-HER2 antibody may be enhanced by the anti-PD-1/PD-L1 mAb by activating the immune system and increasing the infiltration of T cells.

Inetetamab is an anti-HER2 mAb with a more potent ADCC effect than trastuzumab and was approved for the treatment of HER2$^+$ advanced metastatic breast cancer.[19] In this study, we explored the synergistic anti-tumor effect of atezolizumab, an mAb targeting PD-L1, and inetetamab *in vivo* to provide a potential therapeutic strategy for HER2$^+$ OCs.

RESULTS

Anti-HER2 mAb inhibits the growth of HER2$^+$ tumors *in vivo*

We quantified the expression levels of HER2 in three OC cell lines using western blotting (WB), which revealed that SKOV3 cells presented the highest expression level of HER2, followed by ES2 cells. CAOV3 cells barely expressed HER2 (Figure 1A). The immunohistochemistry (IHC) results of the subcutaneous tumors generated from these cells were consistent with the WB results (Figure 1B). The BALB/c nude mice with subcutaneous tumors derived from SKOV3 cells were treated with phosphate-buffered saline (PBS), trastuzumab (10 mg/kg) or inetetamab (10 mg/kg) via tail injection. The growth of tumors from the mice injected with anti-HER2 mAbs was significantly hindered compared with that in the PBS group. There was no difference between the mice treated with trastuzumab and those treated with inetetamab, as expected (Figures 1C and S1A). In a study of melanoma, trastuzumab was reported to upregulate the expression of PD-L1.[20] We wondered whether the same impact could be detected in EOC tumors. IHC was employed to verify the conjecture, which revealed that the HER2 mAbs slightly increased the expression of PD-L1 in SKOV3 cells and that tumors treated with inetetamab presented greater PD-L1 expression than did those treated with trastuzumab (Figure 1D). Similar experiments were conducted in nude mice with subcutaneous tumors derived from CAOV3 and ES2 cells. However, inetetamab did not inhibit the growth of tumors derived from either CAOV3 or ES2 cells. Changes in PD-L1 expression in tumors were detected in both groups of mice (Figures 1E–1H, S1B, and S1C). However, the mean optical densities (ODs) of PD-L1 in CAOV3 and ES2 tumors were extremely low. The changes in the expression of PD-L1 had no biological significance. Both inetetamab and trastuzumab could impede the growth of SKOV3 cells *in vitro* but had no influence on CAOV3 or ES2 cells (Figure S1D). These results suggested that the anti-tumor effect of the anti-HER2 mAb depended on the expression level of HER2 in EOC tumors.

Overexpression of HER2 increases PD-L1 levels in EOC tumors

We next investigated the influence of the anti-HER2 mAb on the expression of PD-L1 in EOC cells. The basal levels of PD-L1 in human EOC cells were detected via WB. The expression of PD-L1 in ES2 cells was considerably higher than that in CAOV3 and SKOV3 cells (Figure 2A). The SKOV3 cells were then treated with different concentrations of inetetamab for 72 h. However, no significant changes in the level of PD-L1 in SKOV3 cells were observed after the treatment of inetetamab (Figure 2B). Lentivirus infection was used to upregulate the protein level of HER2 in HER2$^-$ EOC cells, including ES2, CAOV3, and ID8. The overexpression of HER2 elevated the PD-L1 levels in ES2, CAOV3, and ID8 cells. Unexpectedly, similar to those in SKOV3 cells, no notable alterations in the PD-L1 levels in ES2, CAOV3, or ID8 cells occurred after treatment with anti-HER2 mAbs (Figure 2C). The proliferation abilities of HER2-overexpressing EOC cells, which was up-regulated compared with the NC cells, were evaluated via 5-ethynyl-2′-deoxyuridine (EdU) assays (Figure S2). Compared with those from the ES2-NC group, the tumors from the ES2-HER2 group grew faster *in vivo* (Figure 2D). A higher level of PD-L1 was detected in tumors from the ES2-HER2 group, which is consistent with the IHC results of the tumors derived from the ID8-HER2 and ID8-NC groups (Figure 2E). The difference between the *in vivo* and *in vitro* results suggested that the role of HER2 and the effect of the anti-HER2 mAb may be related to the tumor microenvironment.

Expression of HER2 is positively related to PD-L1 in tumors from EOC patients

It has been reported that only approximately 16% of tumors from EOC patients express HER2.[21] We examined the levels of HER2 and PD-L1 in a cohort of 45 EOC patients. The IHC results showed that the HER2$^+$ tumors had relatively higher levels of PD-L1 than their HER2$^-$ counterparts (Figure 3A). The expression level of HER2 was positively related to the level of PD-L1 in the tumors of EOC patients (Figure 3B). We also assessed the infiltration of T cells in HER2$^+$ and HER2$^-$ EOC tumors. More CD4$^+$ and CD8$^+$ T cells were detected in HER2$^+$ tumors (Figure 3C). Correlation

Figure 1. Anti-HER2 mAb inhibits the growth of HER2$^+$ tumor *in vivo*

(A) Western blot analysis of HER2 in SKOV3, ES2, and CAOV3. (B) Representative images of IHC (HER2) staining of the paraffin-embedded sections (magnification 400×, scale bar: 20 μm). (C) Subcutaneous tumor of SKOV3 after treatment; tumor image (left), dot plot of tumor weight (right). (D) Representative images of IHC (HER2 and PD-L1) staining of the paraffin-embedded sections (left, magnification 400×, scale bar: 20 μm), dot plots of mean ODs (right). (E) Subcutaneous tumor of CAOV3 after treatment; tumor image (left), dot plot of tumor weight (right). (F) Representative images of IHC (HER2 and PD-L1) staining of the paraffin-embedded sections (left, magnification 400×, scale bar: 20 μm), dot plots of mean ODs (right). (G) Subcutaneous tumor of ES2 after treatment; tumor image (left), dot plot of tumor weight (right). (H) Representative images of IHC (HER2 and PD-L1) staining of the paraffin-embedded sections (left, magnification 400×, scale bar: 20 μm), dot plots of mean ODs (right). Data are represented as mean ± SD. p values were calculated using the one-way analysis of variance (C and D) and unpaired t test (E–H). ns, no significance; $^*p < 0.05$; $^{**}p < 0.01$; $^{***}p < 0.001$; $^{****}p < 0.0001$.

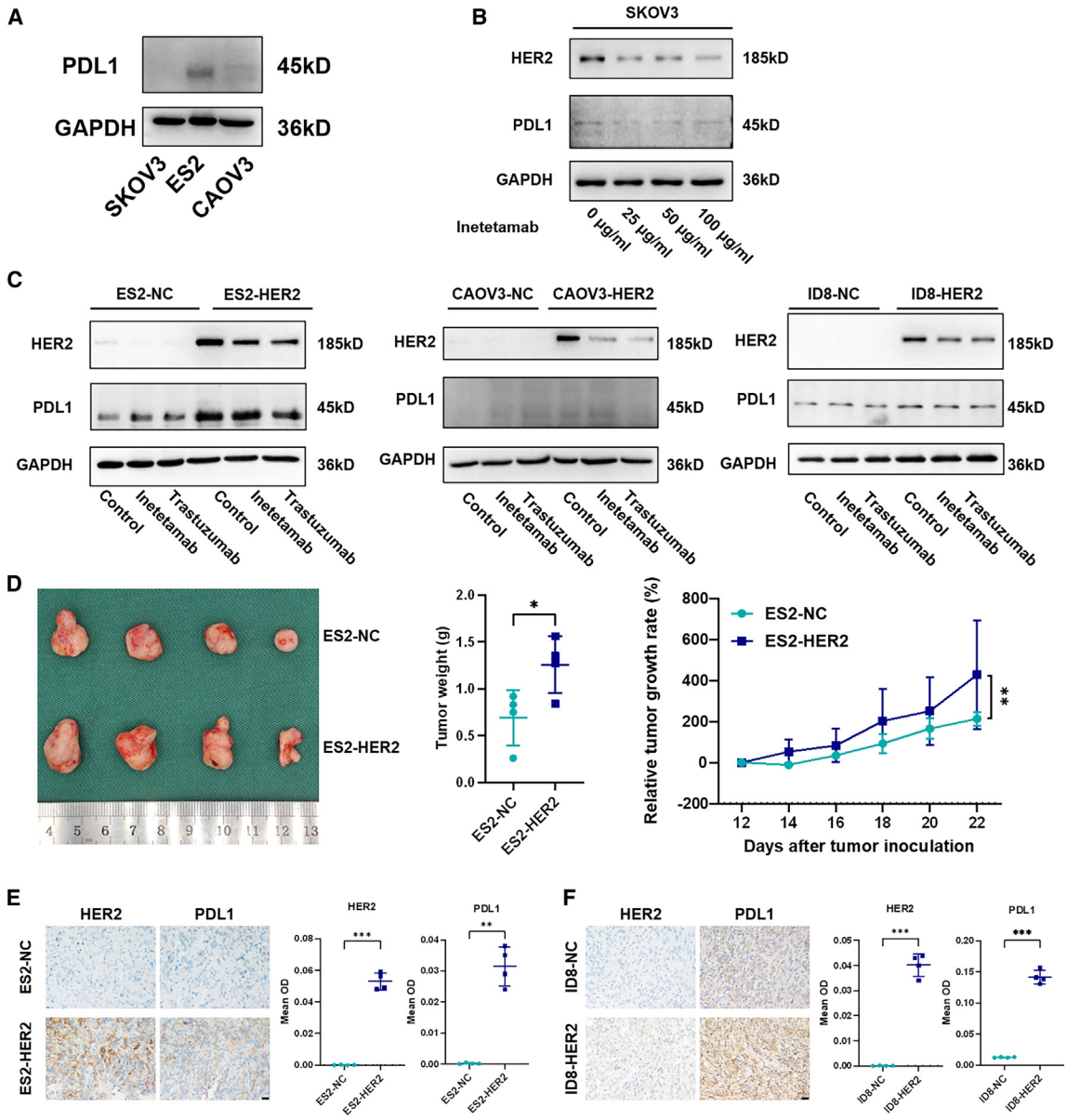

Figure 2. The overexpression of HER2 increases the PD-L1 level in EOC tumor

(A) Western blot analysis of PD-L1 in SKOV3, ES2, and CAOV3. (B) Western blot analysis of HER2 and PDL1 in SKOV3 treated by inetetamab with different concentrations. (C) Western blot analysis of HER2 and PD-L1 in ES2-NC/HER2, CAOV3-NC/HER2, and ID8-NC/HER2 treated by PBS, inetetamab, and trastuzumab. (D) Subcutaneous tumor of ES2-NC and ES2-HER2; tumor image (left), dot plot of tumor weight (center), curve of tumor growth (left). (E) Representative images of IHC (HER2 and PD-L1) staining of the paraffin-embedded sections (left, magnification 400×, scale bar: 20 μm), dot plots of mean ODs (right). (F) Representative images of IHC (HER2 and PD-L1) staining of the paraffin-embedded sections (left, magnification 400×, scale bar: 20 μm), dot plots of mean ODs (right). Data are represented as mean ± SD. *p* values were calculated using unpaired t test (D) or Welch's t test (E and F). $^{*}p < 0.05$; $^{**}p < 0.01$; $^{***}p < 0.001$.

analysis revealed that the expression of HER2 was positively related to the infiltration of both $CD4^{+}$ and $CD8^{+}$ T cells and that the same was true for PD-L1 (Figure 3D). Furthermore, the correlations between the expression of HER2 or PD-L1 and the clinicopathological paraments of our cohort were analyzed. Patients receiving preoperative chemotherapy exhibited increased expression of PD-L1 and HER2 (Table 1). However, the expressions of HER2 demonstrated no significant statistical difference, which may be attributed to the limitation of the size of the cohort. No obvious differences in the expression of HER2 or PD-L1 were observed in the patients with different ages, FIGO (International Federation of Gynecology and Obstetrics) stages, histological types, metastases, or the expression

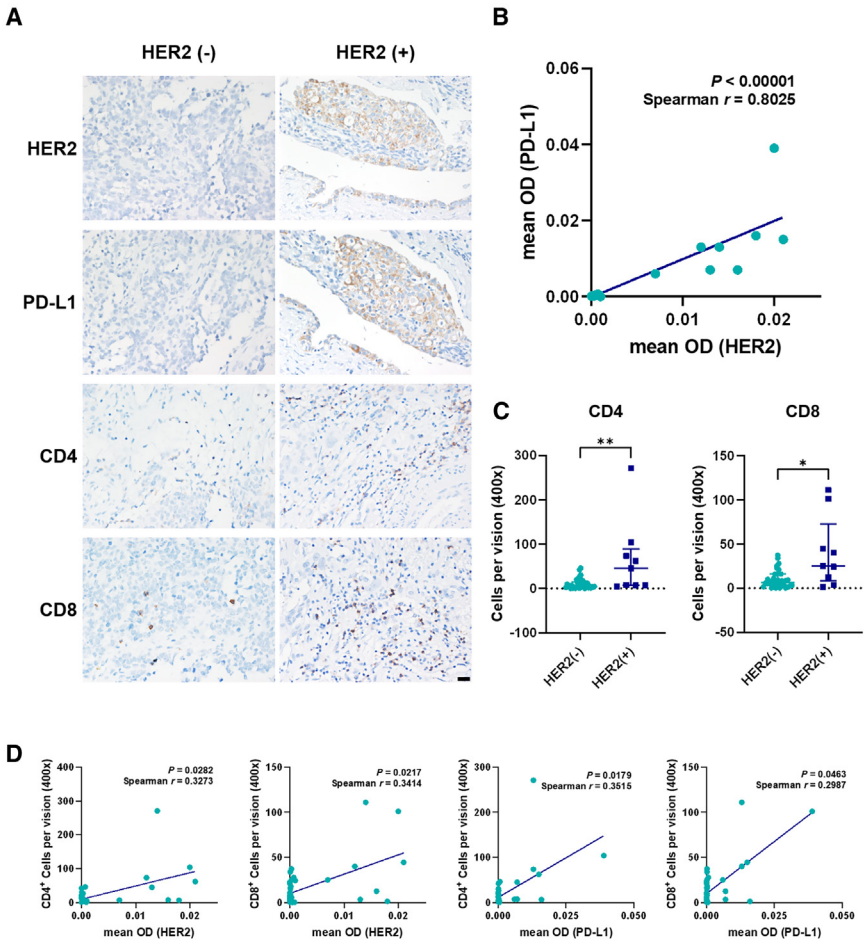

Figure 3. The expression of HER2 is positively related to PD-L1 in tumors from EOC patients

(A) Representative images of IHC (HER2, PD-L1, CD4, and CD8) staining of the ovarian cancer tumors from patients (magnification 400×, scale bar: 20 μm). (B) Correlation analysis of mean ODs between HER2 and PD-L1 in the ovarian cancer tumors from patients. (C) Dot plots of the infiltration of $CD4^+$ and $CD8^+$ cells in tumors from patients with different expression of HER2. Data are represented as median with interquartile range. (D) Correlation analysis of the mean ODs (HER2 and PD-L1) and the cell infiltrations ($CD4^+$ and $CD8^+$ cells) in ovarian cancer tumors from patients. *p* values were calculated using Spearman correlation analysis (B and D) or Mann-Whitney test (C). $^*p < 0.05$; $^{**}p < 0.01$.

models of P53, WT1, and Ki67. The correlation of HER2 and PD-L1 in EOC tumors provides the prerequisites for the combination of an HER2 mAb and a PD-L1 mAb. The EOC patients who have received preoperative chemotherapy may be a beneficiary of combined therapy.

Inetetamab combined with atezolizumab inhibits the progress of HER2$^+$ tumors *in vivo* with a long-term effect

Finally, we evaluated the anti-tumor effects of the mAbs targeting HER2 and PD-L1 *in vivo*. ID8-HER2 was used to construct a peritoneal dissemination model in C57BL/6N mice. The tumor-bearing mice were divided into four groups and were injected with PBS, inetetamab, atezolizumab (an anti-PD-L1 mAb), or both inetetamab and atezolizumab according to their groups. The growth of the tumors was monitored by *in vivo* imaging. Inetetamab alone could initially suppress the growth of the tumors, but the suppression weakened after 2 weeks of treatment. The utilization of atezolizumab inhibited the progress of tumors, while the effect was reduced after 1 week of stopping the treatment. The progress of tumors in the mice was significantly impeded by the combined treatment of inetetamab and atezolizumab. Moreover, the tumors of the mice treated with both inetetamab and atezolizumab were continuously suppressed even 2 weeks after the termination of mAb administration (Figure 4A). Meanwhile, there was no significant change in the body weights of the mice in each group during the *in vivo* experiment, which suggested that the treatment did not have significant toxicity (Figure S3). The $Ki67^+$ cell ratio was evaluated via IHC, which indicated that tumors treated with inetetamab combined with atezolizumab presented a low ratio of $Ki67^+$ cells, but there was no difference between the single-drug-treated and the combined-drug-treated mice (Figure 4B). These findings suggested that the combination did not enhance the inhibition of tumor proliferation compared to the drug alone. IHC was also employed to analyze the infiltration of T cells, which demonstrated that either inetetamab or atezolizumab increased the infiltration of $CD8^+$ T cells, yet the infiltration of $CD4^+$ T cells did not differ between the single-drug-treated mice and their control counterparts. However, the combination of inetetamab and atezolizumab significantly raised the number of both $CD4^+$ and $CD8^+$ T cells in the tumor, which exceeded those in the single-drug groups (Figure 4B). GZMB and PRF1 are the key effector factors involved in the anti-tumor effects of $CD8^+$ T cells. The expressions of GZMB and PRF1 were detected by IHC, which revealed that the combination of inetetamab and atezolizumab significantly increased the number of both $GZMB^+$ and $PRF1^+$ cells in the tumor, which is higher than those in the single-drug groups (Figures 5A and 5B). These results indicated that the combination of inetetamab and atezolizumab could inhibit the growth of $HER2^+$ EOC tumors *in vivo* and induce a long-term anti-tumor effect. Tissue-resident memory T cells, which are identified as $CD103^+CD8^+$ cells, were believed to play a key role in long-term tumor suppression. Multiplexed IHC (mIHC) was utilized to evaluate the infiltration of tissue-resident memory T cells in the tumors from the mice in each group. The infiltration of $CD103^+CD8^+$ cells was increased in the tumors from mice treated with the combination of inetetamab and atezolizumab

Table 1. Correlation between the expression of HER2 or PD-L1 and the clinicopathological parameters in tumors from EOC patients

Parameters	N	HER2 (mean OD, median [IQR])	p[a]	PD-L1 (mean OD, median [IQR])	p[a]
Age, y					
<55	21	0.0000254 (0.0000048, 0.0039310)	0.30940	0.0000397 (0.0000030, 0.0031995)	0.63957
≥55	24	0.0000804 (0.0000237, 0.0003320)	–	0.0000834 (0.0000174, 0.0001610)	–
FIGO stage					
I–II	7	0.0001320(0.0000488, 0.0003765)	0.41550	0.0000648 (0.0000172, 0.0002552)	0.86324
III–IV	38	0.0000684(0.0000083, 0.0006940)	–	0.0000803 (0.0000123, 0.0002270)	–
Preoperative chemotherapy					
Yes	8	0.0002875 (0.0000499, 0.0190000)	0.05364	0.0001535 (0.0001225, 0.0155000)	0.02404
No	37	0.0000622 (0.0000083, 0.0003320)	–	0.0000435 (0.0000054, 0.0001630)	–
Histological type					
Type II	38	0.0000684 (0.0000094, 0.0003320)	0.82648	0.0000803 (0.0000126, 0.0002270)	0.35553
Non-type II	7	0.0001320 (0.0000213, 0.0007105)	–	0.0000145 (0.0000029, 0.0002552)	–
Omental metastasis					
Yes	30	0.0000554 (0.0000080, 0.0003040)	0.23925	0.0001050 (0.0000125, 0.0001950)	0.55622
No	15	0.0001117 (0.0000354, 0.0006940)	–	0.0000591 (0.0000054, 0.0004270)	–
Lymph node metastasis					
Yes	17	0.0001750 (0.0000153, 0.0070000)	0.88543	0.0000142 (0.00001400, 0.006000)	0.37745
No	17	0.0000780 (0.0000238, 0.0005575)	–	0.0000661 (0.0000136, 0.0002865)	–
Unknown[b]	11	–	–	–	–
Appendiceal metastasis					
Yes	14	0.0001277 (0.0000138, 0.0003040)	0.78100	0.0001430 (0.0000554, 0.0001950)	0.33042
No	24	0.0000755 (0.0000115, 0.0009310)	–	0.0000435 (0.0000090, 0.0005170)	–
Unknown[b]	7	–	–	–	–
P53					
Wild type	9	0.0003120 (0.0000622, 0.0004210)	0.44067	0.0000648 (0.0000145, 0.0001630)	0.64152
Mutation type	35	0.0000642 (0.0000089, 0.0004950)	–	0.0000933 (0.0000125, 0.0003130)	–
Untested[c]	1	–	–	–	–
WT1					
Positive	32	0.0000684 (0.0000089, 0.0007780)	0.95008	0.0000992 (0.0000126, 0.0005170)	0.21509
Negative	13	0.0001320 (0.0000109, 0.0003320)	–	0.0000290 (0.0000022, 0.0001610)	–
Ki67 (LI)					
≤50%	9	0.0000726 (0.0000083, 0.0070000)	0.70608	0.0000933 (0.0000126, 0.0060000)	0.75926
>50%	20	0.0000859 (0.0000550, 0.0005575)	–	0.0001250 (0.0000305, 0.0004130)	–
Untested[c]	16	–	–	–	–

FIGO, International Federation of Gynecology and Obstetrics; IQR, interquartile range; LI, labeling index; OD, optical density.
[a]p values were calculated using the Mann-Whitney test.
[b]The patients did not undergo lymphadenectomy or appendectomy.
[c]The samples from patients were not tested for P53 or Ki67.

(Figure 5C). These findings suggested that the combination treatment induced the long-term anti-tumor effect by recruiting $CD103^+CD8^+$ cells into tumors.

DISCUSSION

ERBB2, which encodes the protein HER2, is one of the oncogenes in several cancers, such as breast cancer, gastric cancer, and lung cancer.[22] Approximately 30% of breast cancer patients have a positive expression of HER2.[23] In contrast, it is reported that the $HER2^+$ percentage in OC patients is only approximately 16%, mostly presenting with mild staining,[21] which imposes restrictions on the utilization of anti-HER2 mAbs in the treatment of OC. In the present study, the expressions of HER2 in OC tissues were analyzed via IHC,[24] which suggested that HER2 could be detected in 20% of OC patients. In our

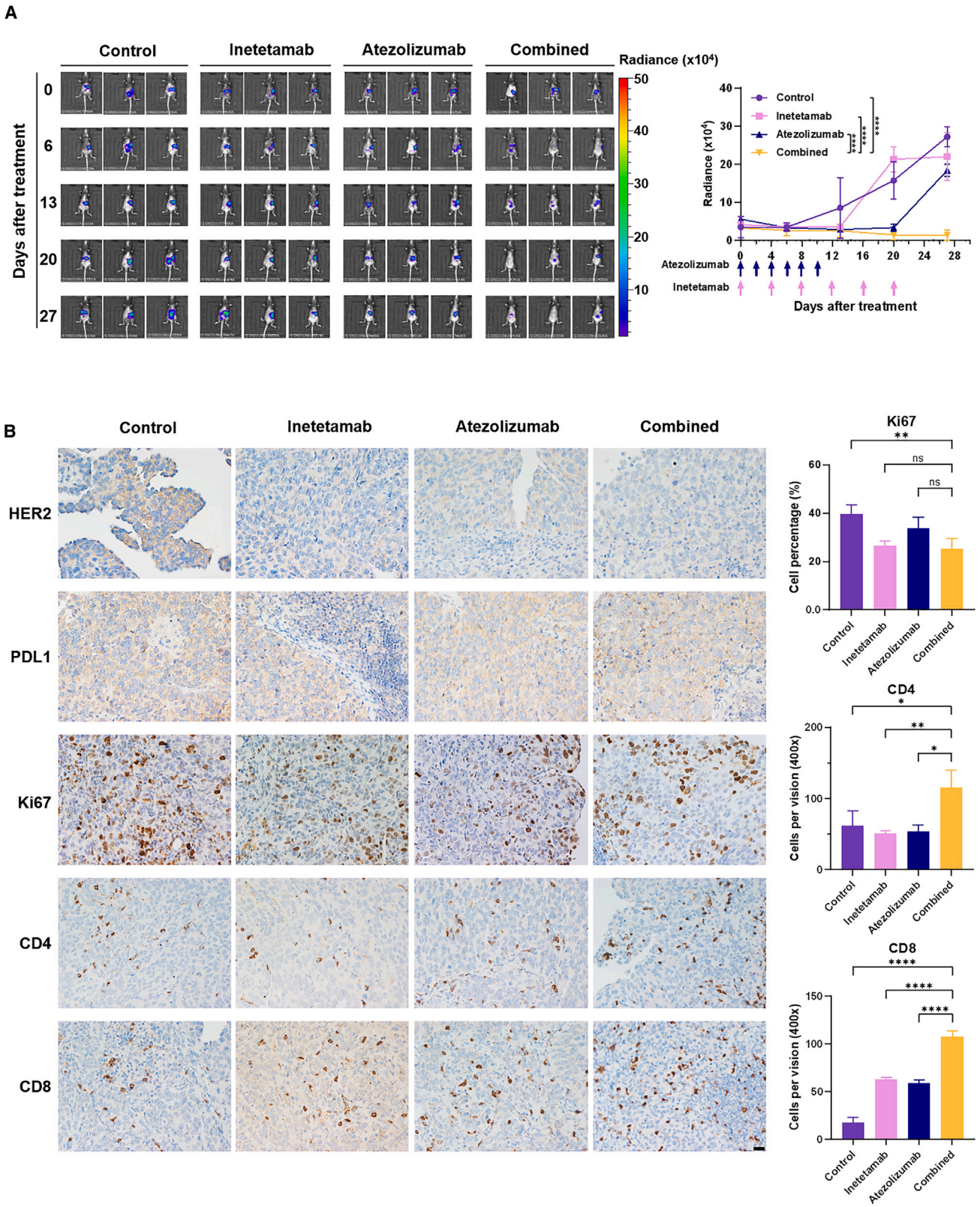

(legend on next page)

cohort, 15.6% of the patients had an IHC score of 2+, and no patients had an IHC score of 3+.

Trastuzumab is the first HER2-targeted drug, and it is directed against the extracellular domain of HER2.[25] Fujimura et al. reported that the utilization of trastuzumab could inhibit tumor growth and prolong the survival of OC tumor-bearing mice and that the extent of the effect of trastuzumab was dependent on the HER2 expression level.[26] Similar results were observed in our study. Although several clinical trials failed to validate any beneficial effect of treatment with trastuzumab and related anti-HER2 mAbs in $HER2^{-}$ or $HER2^{low}$ breast cancer, a small number of $HER2^{low}$ patients achieved a response.[27–29] The response rates to the single-agent trastuzumab and pertuzumab in OC are only 7% and 4.3%, respectively,[8,9] which was partly attributed to the low frequency of HER2 overexpression. In recent decades, research efforts have been made to improve the effectiveness of anti-HER2 therapies. Antibody-drug conjugates are one of the tactics used to overcome the defects of classical anti-HER2 mAbs. Several clinical trials have shown that patients with low HER2 expression levels can benefit from the antibody-drug conjugates targeting HER2,[30] which indicates that treatments targeting HER2 can still be used in patients with low HER2 expression.

Trastuzumab is able to suppress intracellular HER2-mediated signal transductions, the ADCC and the antibody-dependent cellular phagocytosis.[31,32] Inetetamab is an anti-HER2 mAb with the same binding site as trastuzumab but a more potent ADCC effect than trastuzumab.[19] In the *in vitro* assay, trastuzumab and inetetamab significantly impeded the growth of SKOV3 cells with high expressions of HER2. In addition, the inhibitory effect of inetetamab on tumors is slightly greater than that of trastuzumab *in vivo*, yet the difference is not statistically significant. More tests should be performed to compare the effects of inetetamab and trastuzumab in OC with low levels of HER2.

PD-1 and PD-L1 are a pair of immune checkpoints. Inhibitors of PD-1/PD-L1 have been widely used to treat cervical cancer and endometrial cancer. However, the application of PD-1/PD-L1 blockers in OC is limited, and the underlying reason and mechanism are still unclear. The co-expression of HER2 and PD-L1 has been observed in human gastric cancer.[33] Treatment with trastuzumab can increase the HER2 expression of NK cells in $HER2^{+}$ breast cancer patients.[32] We also found that treatment with an anti-HER2 mAb increased the expression of PD-L1 in tumors derived from SKOV3 cells. Moreover, the IHC results demonstrated that the expression level of HER2 was positively related to the level of PD-L1 in the tumors of EOC patients. Correlation analysis revealed that patients who received preoperative chemotherapy had increased expression of PD-L1 and HER2, which suggested that these patients were more likely to benefit from combined therapy. Biomarkers that are associated with the treatment efficacy of immune checkpoint inhibitors, such as blood count and albumin level, could also be useful for screening subgroups of patients who may be suitable for the therapy.[34] In future research, we will incorporate additional metrics to stratify patients. Margetuximab, a HER2-targeted mAb, can enhance the ADCC effect *in vitro*, which is mediated by T cells and dependent on HER2.[11] This finding suggested a prospective anti-tumor effect of the combination of anti-PD-1/PD-L1 and anti-HER2 treatments, which markedly inhibited tumors in $HER2^{+}$ gastric cancer.[35] We constructed a peritoneal dissemination model in C57BL/6N mice with HER2-overexpressing ID8 cells and found that the combined use of atezolizumab and inetetamab could suppress the growth of tumors *in vivo*. The side effects induced by immune checkpoint inhibitors, such as hepatitis, pneumonia, and colitis, have been reported previously, and some biomarkers, such as the aspartate aminotransferase and the alanine aminotransferase, have been reported to be useful for predicting and monitoring the side effects during therapy.[36] The body weights of the mice did not change significantly during the *in vivo* test, suggesting a certain degree of safety of the drug combination. However, additional testing is recommended to evaluate further the safety of combination therapy.

Moreover, a long-term anti-tumor effect was observed in the mice receiving the combined treatment. The long-term anti-tumor effect is an acquired immune effect mediated by memory T cells, which are composed of central memory T cells, effective memory T cells, stem memory T cells, and tissue-resident memory T cells.[37] Tissue-resident memory T cells are a subset of $CD8^{+}$ T cells with longevity and the capacity to coordinate rapid immune responses[38] and can be identified as $CD103^{+}CD8^{+}$ cells. IHC analysis revealed that the combination of inetetamab and atezolizumab significantly increased the infiltration of $CD8^{+}$ T cells and $CD103^{+}CD8^{+}$ cells in tumors, which was higher than that in the single-drug groups. This finding suggests that the combination treatment could induce the long-term anti-tumor effect possibly by recruiting tissue-resident memory T cells into the tumor. However, the exact mechanism needs further investigation, and methods to activate tissue-resident memory T cells may constitute a strategy to increase the efficacy of combination treatment in the future.

There are also several limitations to this work. For example, a mouse-specific mAb should be a better choice considering the mouse model used in the *in vivo* test. Owing to the lower $HER2^{+}$ ratio in EOC patients, the size of cohort is another limitation for this research. Future studies could include more patients to expand the size of the cohort. In conclusion, this research provides preclinical evidence that

Figure 4. Inetetamab combined with atezolizumab inhibits the progress of $HER2^{+}$ tumors *in vivo* with a long-term effect

(A) BLI image of peritoneal dissemination model of ID8-HER2 cells with different treatments. Right: the curves of tumor burden by BLI; data are represented as mean ± SD. (B) Representative images of IHC (HER2, PD-L1, Ki67, CD4, and CD8) staining of the omentum from mice (left, magnification 400×, scale bar: 20 μm). Bar plots of the infiltration of $CD4^{+}$ and $CD8^{+}$ cells and the ratio of $Ki67^{+}$ cells in the omentum from the mice (right). Data are represented as mean ± SD. *p* values were calculated using the one-way (B) or two-way (A) analysis of variance. $^{*}p < 0.05$; $^{**}p < 0.01$; $^{***}p < 0.001$; $^{****}p < 0.0001$.

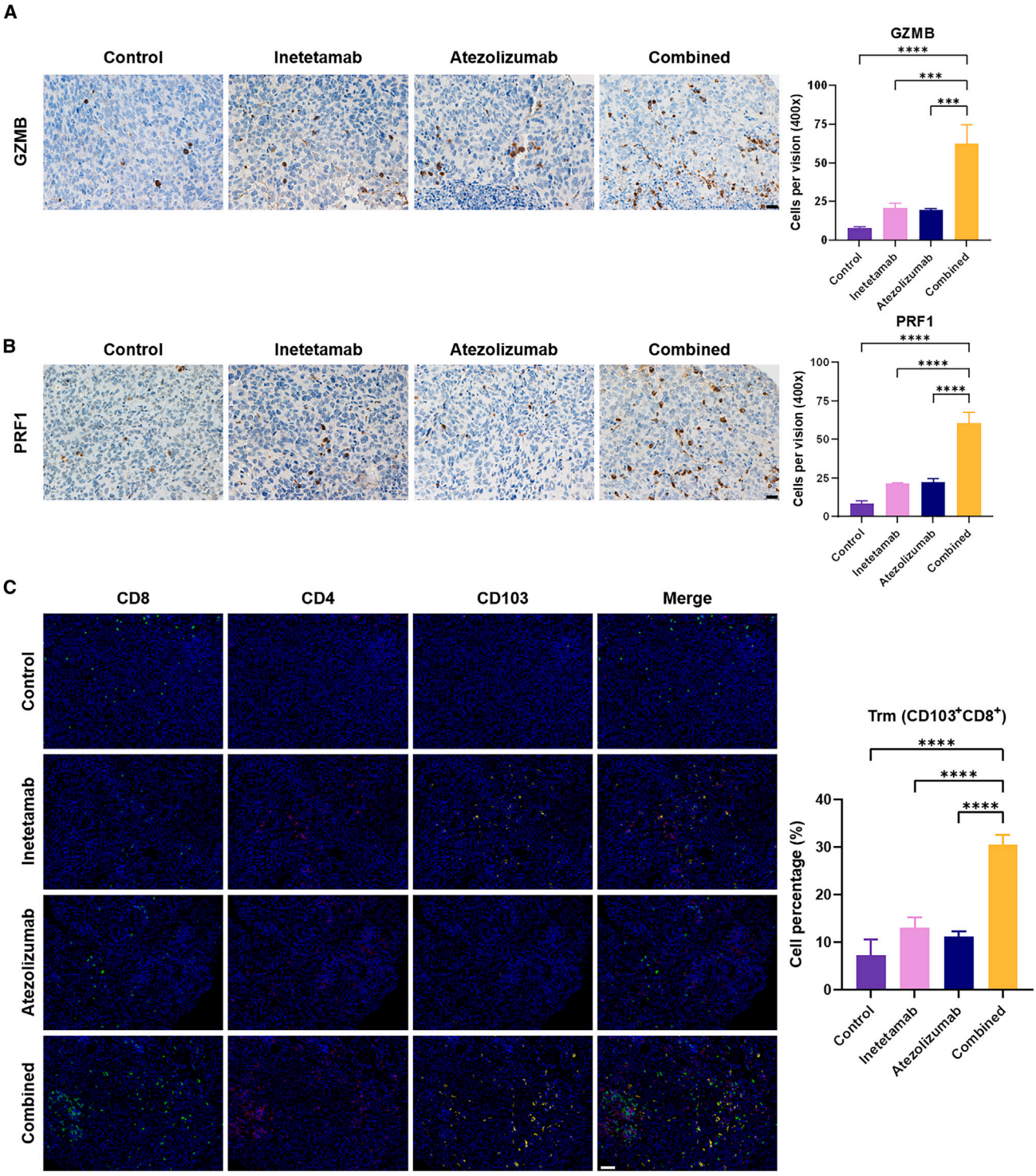

Figure 5. The infiltration of CD103$^+$CD8$^+$ T cells was increased in the omentum of mice treated by inetetamab along with atezolizumab

(A and B) Representative images of IHC (GZMB and PRF1) staining of the omentum from mice (left, magnification 400×, scale bar: 20 μm). Data are represented as mean ± SD. (C) Representative images of mIHC staining of the omentum from mice (left, magnification 400×, scale bar: 25 μm). *p* values were calculated using the one-way analysis of variance. ***$p < 0.001$; ****$p < 0.0001$.

combining the administration of anti-HER2 and anti-PD-L1 agents is a potential treatment strategy for EOC patients.

MATERIALS AND METHODS

Cell lines

The human OC cell lines ES2, SKOV3, and CAOV3 were purchased from the China Center for Type Culture Collection (Wuhan). The murine OC cell line ID8 expressing firefly luciferase was a gift from Xiao Haihua's laboratory (Chinese Academy of Sciences, Beijing). All cells were cultured in Dulbecco's Modified Eagle's Medium/F12 medium (catalog no. L310KJ, BasalMedia Technologies, Shanghai, China) supplemented with 10% fetal bovine serum (catalog no. BC-SE-FBS01, Biochannel, Nanjing, China). For subcutaneous inoculation, cells were collected in a logarithmic growth phase. The cells were authenticated using short tandem repeat profiling within 1 year. All cells were free of mycoplasma. The HER2-overexpressing cell lines were constructed using the lentivirus expressing HER2 cDNA (GeneChem, Shanghai, China) with a multiplicity of infection of 10, and an NC (negative control)-lentiviral vector was used as negative control. Blasticidin S (catalog no. S180J0, BasalMedia Technologies, Shanghai, China) was used to eliminate uninfected cells with a concentration of 100 μg/mL for 6 days.

Human subjects

The research was approved by the Ethics Committee of Union Hospital, Tongji Medical College, Huazhong University of Science and Technology. Informed consent was obtained from all patients.

Animals

Female BALB/c nude mice aged 4 weeks (Charles River Laboratories, Beijing, China) and female C57BL/6N mice aged 4 weeks (Charles River Laboratories, Beijing, China) were housed under specific pathogen-free conditions. All animal experiments were conducted at the Laboratory Animal Center at the Wuhan Youdu Biotechnology Company and approved by the Institutional Animal Care and Use Committee at Wuhan Youdu Biotechnology Company. The tumor cells were used to build subcutaneous tumor models by injecting 5×10^6 cells per mouse. Tumor growth and body weights of mice were recorded every 2 days. The anti-HER2 mAbs or PBS were administered via peritoneal injection when the volume of tumors reached 500–800 mm^3 according to their groups. The dose of anti-HER2 mAbs was 10 mg/kg every 2 days. All mice were euthanized when the diameter of the largest tumor reached 2 cm or after 6 times the drug administration. For the peritoneal dissemination model, ID8-HER2 cells were injected intraperitoneally (i.p.) at 10^7 per mouse. After 1 week, the mice were divided into four groups randomly and treated with drugs according to their groups. The initial dose of inetetamab was 4 mg/kg and the maintenance dose was 2 mg/kg every 4 days. The dose of atezolizumab was 1 mg/kg every 2 days.

IHC

Tissues were fixed in formalin and embedded in paraffin, and the sections were used for IHC. For IHC, the sections were subjected to heat-mediated antigen retrieval in pH 6.0 citrate buffer or pH 9.0 Tris-EDTA buffer after routine deparaffinization and rehydration, according to the the protocols of the antibodies for the IHC test. The following staining steps were conducted using a rabbit biotin-streptavidin horseradish peroxidase detection system (catalog no. 36312ES50, Yeasen Biotechnology, Shanghai, China). The staining images of tumor tissues were evaluated by the IHC toolbox ImageJ (NIH, Bethesda, MD). The primary antibodies used were hHER2 (human HER2; 1:200, catalog no. A21248, Abclonal, Wuhan, China), hPD-L1 (1:200, catalog no. A19135, Abclonal, Wuhan, China), mPD-L1 (murine PD-L1; 1:200, catalog no. A21443, Abclonal, Wuhan, China), hCD4 (1:400, catalog no. ab133616, Abcam, Cambridge, UK), mCD4 (1:800, catalog no. ab183685, Abcam, Cambridge, UK), hCD8 (1:1,000, catalog no. ab237709, Abcam, Cambridge, UK), mCD8 (1:2,000, catalog no. ab217344, Abcam, Cambridge, UK), mGZMB (1:200, catalog no. 46890, Cell Signaling Technology, Danvers, MA), and mPRF1 (1:200, catalog no. 31647, Cell Signaling Technology, Danvers, MA). Finally, the sections were counterstained with hematoxylin & eosin.

Bioluminescent imaging

Disease progression was monitored by bioluminescent imaging (BLI) on an *in vivo* imaging system (IVIS, Lumina II, Caliper Life Science, Hopkinton, MA) every 3 days. The firefly luciferase substrate D-luciferin potassium salt (catalog no. HY12505, HYCEZMBIO, Wuhan, China) was intraperitoneally injected into the mice at a dose of 150 mg/kg 15 min before imaging. During imaging, isoflurane was administered to keep the mice anesthetized. The radiance value was measured by Living Image software (version 4.3.1, Caliper Life Science) using the region of interest tools.

EdU assay

A Cell-Light EdU kit (catalog no. C10310-1, RiboBio, Guangzhou, China) was used to detect the proliferative proportion of cancer cells. The assay was conducted following the manufacturer's instructions. Fluorescent images were captured at a magnification of 200× or 400×. At least 10 images were captured for each sample. EdU^+ cell (red) numbers and total cell (blue) numbers were counted, and the average EdU^+ ratio was calculated for each sample. The assays were performed in triplicate.

Methylthiazolyldiphenyl-tetrazolium bromide assay

Cells were seeded in the 96-well plate, with a density of 1,000 cells/well and cultured for 24 h. Fresh medium with anti-HER2 mAb was added to the plate, with concentrations of 0, 2, 4, 5, and 8 μg/mL. The cells were incubated for the next 72 h. Methylthiazolyldiphenyl-tetrazolium bromide (catalog no. M8180, Solarbio, Beijing, China) was added to the plate, with a final concentration of 1 mg/mL. The supernatant fluid was abandoned and dimethyl sulfoxide (catalog no. BS087, Biosharp, Hefei, China) was added to the plate, with a volume of 200 μL/well after 4 h. The absorbances were detected using the microplate reader (SpectraMax i3x, Molecular Devices, San Jose, CA), with a λ of 570 nm. Each experiment was performed in triplicate.

WB

For cell lysate, total cellular proteins were extracted by radioimmunoprecipitation assay (P0013B, Beyotime, Shanghai, China) with 1% cocktail (P8340, Sigma-Aldrich, St. Louis, MO). Proteins were quantified by bicinchoninic acid assay (catalog no. P10012, Beyotime, Shanghai, China), and 15 μg of each sample was loaded for the blotting process. The primary antibodies used were HER2 (1:1,000, catalog no. A21248, Abclonal, Wuhan, China), GAPDH (1:10,000, catalog no. A19056, Abclonal, Wuhan, China), and PD-L1 (1:1,000, catalog no. A21443, Abclonal, Wuhan, China). Each experiment was performed in triplicate. The original WBs are presented in Figures S4 and S5.

mIHC

The 5-μm-thick sections from tissues fixed in formalin and embedded in paraffin were used for mIHC. The process was conducted with a tyramine signal amplification kit (Wuhan Pigeon Biotechnology, Wuhan, China) according to the manufacturer's protocol. The primary antibodies were mCD4 (1:1,000, catalog no. ab183685, Abcam, Cambridge, UK), mCD8 (1:2,000, catalog no. ab217344, Abcam, Cambridge, UK), and mCD103 (1:5,000, catalog no. ab224202, Abcam, Cambridge, UK). DAPI was used for nuclear counterstaining. Pannoramic MIDI (3DHISTECH, Budapest, Hungary) was used to capture the images and identify all markers of interest.

Quantification and statistical analysis

GraphPad Prism 9.4 and R 4.1.3 were used to perform all statistical analyses. All data are presented as the mean ± standard deviation or in quartiles. The differences between the two groups were analyzed by unpaired or paired t test, Welch's t test, or Mann-Whitney test. The differences among more than three groups were analyzed by one-way or two-way analysis of variance. The correlation between the two groups was analyzed by Pearson correlation analysis. The results were considered to be statistically significant at $p < 0.05$. More details are provided in the figure captions.

DATA AND CODE AVAILABILITY

All raw and analyzed data supporting the findings of this study are available upon request.

ACKNOWLEDGMENTS

This work was supported by the Key Research and Development Program of Hubei Province [2021BCA118].

AUTHOR CONTRIBUTIONS

Conceptualization, F.Y., X.Z., Q.Z., and Y.Z. Methodology, F.Y., X.Z., M.C., L.H., and L.G. Formal analysis, F.Y., X.Z., and L.G. Investigation, F.Y., X.Z., M.C., and L.H. Resources, Q.Z. and Y.Z. Writing – original draft, F.Y. and X.Z. Writing – review & editing, F.Y., Q.Z., and Y.Z. Supervision, Y.Z. Project administration, Q.Z. Funding acquisition, Y.Z.

DECLARATION OF INTERESTS

The authors declare no competing interests.

SUPPLEMENTAL INFORMATION

Supplemental information can be found online at https://doi.org/10.1016/j.omton.2025.200938.

REFERENCES

1. Siegel, R.L., Giaquinto, A.N., and Jemal, A. (2024). Cancer statistics, 2024. CA A Cancer J. Clin. *74*, 12–49. https://doi.org/10.3322/caac.21820.

2. Terry, K.L., Schock, H., Fortner, R.T., Hüsing, A., Fichorova, R.N., Yamamoto, H.S., Vitonis, A.F., Johnson, T., Overvad, K., Tjønneland, A., et al. (2016). A Prospective Evaluation of Early Detection Biomarkers for Ovarian Cancer in the European EPIC Cohort. Clin. Cancer Res. *22*, 4664–4675. https://doi.org/10.1158/1078-0432.CCR-16-0316.

3. Mathieu, K.B., Bedi, D.G., Thrower, S.L., Qayyum, A., and Bast, R.C. (2018). Screening for ovarian cancer: imaging challenges and opportunities for improvement. Ultrasound Obstet. Gynecol. *51*, 293–303. https://doi.org/10.1002/uog.17557.

4. Gradishar, W.J., Moran, M.S., Abraham, J., Abramson, V., Aft, R., Agnese, D., Allison, K.H., Anderson, B., Burstein, H.J., Chew, H., et al. (2023). NCCN Guidelines® Insights: Breast Cancer, Version 4.2023. J. Natl. Compr. Cancer Netw. *21*, 594–608. https://doi.org/10.6004/jnccn.2023.0031.

5. Ajani, J.A., D'Amico, T.A., Bentrem, D.J., Chao, J., Cooke, D., Corvera, C., Das, P., Enzinger, P.C., Enzler, T., Fanta, P., et al. (2022). Gastric Cancer, Version 2.2022, NCCN Clinical Practice Guidelines in Oncology. J. Natl. Compr. Cancer Netw. *20*, 167–192. https://doi.org/10.6004/jnccn.2022.0008.

6. Reibenwein, J., and Krainer, M. (2008). Targeting signaling pathways in ovarian cancer. Expert Opin. Ther. Targets *12*, 353–365. https://doi.org/10.1517/14728222.12.3.353.

7. Slamon, D.J., Godolphin, W., Jones, L.A., Holt, J.A., Wong, S.G., Keith, D.E., Levin, W.J., Stuart, S.G., Udove, J., Ullrich, A., et al. (1989). Studies of the HER-2/neu Proto-Oncogene in Human Breast and Ovarian Cancer. Science *244*, 707–712. https://doi.org/10.1126/science.2470152.

8. Bookman, M.A., Darcy, K.M., Clarke-Pearson, D., Boothby, R.A., and Horowitz, I.R. (2003). Evaluation of monoclonal humanized anti-HER2 antibody, trastuzumab, in patients with recurrent or refractory ovarian or primary peritoneal carcinoma with overexpression of HER2: a phase II trial of the Gynecologic Oncology Group. J. Clin. Oncol. *21*, 283–290. https://doi.org/10.1200/JCO.2003.10.104.

9. Gordon, M.S., Matei, D., Aghajanian, C., Matulonis, U.A., Brewer, M., Fleming, G.F., Hainsworth, J.D., Garcia, A.A., Pegram, M.D., Schilder, R.J., et al. (2006). Clinical activity of pertuzumab (rhuMAb 2C4), a HER dimerization inhibitor, in advanced ovarian cancer: potential predictive relationship with tumor HER2 activation status. J. Clin. Oncol. *24*, 4324–4332. https://doi.org/10.1200/JCO.2005.05.4221.

10. Makhija, S., Amler, L.C., Glenn, D., Ueland, F.R., Gold, M.A., Dizon, D.S., Paton, V., Lin, C.-Y., Januario, T., Ng, K., et al. (2010). Clinical activity of gemcitabine plus pertuzumab in platinum-resistant ovarian cancer, fallopian tube cancer, or primary peritoneal cancer. J. Clin. Oncol. *28*, 1215–1223. https://doi.org/10.1200/JCO.2009.22.3354.

11. Musolino, A., Gradishar, W.J., Rugo, H.S., Nordstrom, J.L., Rock, E.P., Arnaldez, F., and Pegram, M.D. (2022). Role of Fcγ receptors in HER2-targeted breast cancer therapy. J. Immunother. Cancer *10*, e003171. https://doi.org/10.1136/jitc-2021-003171.

12. Schoutrop, E., Moyano-Galceran, L., Lheureux, S., Mattsson, J., Lehti, K., Dahlstrand, H., and Magalhaes, I. (2022). Molecular, cellular and systemic aspects of epithelial ovarian cancer and its tumor microenvironment. Semin. Cancer Biol. *86*, 207–223. https://doi.org/10.1016/j.semcancer.2022.03.027.

13. Bagchi, S., Yuan, R., and Engleman, E.G. (2021). Immune Checkpoint Inhibitors for the Treatment of Cancer: Clinical Impact and Mechanisms of Response and Resistance. Annu. Rev. Pathol. *16*, 223–249. https://doi.org/10.1146/annurev-pathol-042020-042741.

14. Di Federico, A., Mosca, M., Pagani, R., Carloni, R., Frega, G., De Giglio, A., Rizzo, A., Ricci, D., Tavolari, S., Di Marco, M., et al. (2022). Immunotherapy in Pancreatic Cancer: Why Do We Keep Failing? A Focus on Tumor Immune Microenvironment, Predictive Biomarkers and Treatment Outcomes. Cancers *14*, 2429. https://doi.org/10.3390/cancers14102429.

15. Matulonis, U.A., Shapira-Frommer, R., Santin, A.D., Lisyanskaya, A.S., Pignata, S., Vergote, I., Raspagliesi, F., Sonke, G.S., Birrer, M., Provencher, D.M., et al. (2019). Antitumor activity and safety of pembrolizumab in patients with advanced recurrent ovarian cancer: results from the phase II KEYNOTE-100 study. Ann. Oncol. *30*, 1080–1087. https://doi.org/10.1093/annonc/mdz135.

16. Disis, M.L., Taylor, M.H., Kelly, K., Beck, J.T., Gordon, M., Moore, K.M., Patel, M.R., Chaves, J., Park, H., Mita, A.C., et al. (2019). Efficacy and Safety of Avelumab for Patients With Recurrent or Refractory Ovarian Cancer: Phase 1b Results From the JAVELIN Solid Tumor Trial. JAMA Oncol. *5*, 393–401. https://doi.org/10.1001/jamaoncol.2018.6258.

17. Lin, W., Zhang, Y., Yang, Y., Lin, B., Zhu, M., Xu, J., Chen, Y., Wu, W., Chen, B., Chen, X., et al. (2023). Anti-PD-1/Her2 Bispecific Antibody IBI315 Enhances the Treatment Effect of Her2-Positive Gastric Cancer through Gasdermin B-Cleavage Induced Pyroptosis. Adv. Sci. *10*, e2303908. https://doi.org/10.1002/advs.202303908.

18. Chen, Y.-L., Cui, Y., Liu, X., Liu, G., Dong, X., Tang, L., Hung, Y., Wang, C., and Feng, M.-Q. (2021). A bispecific antibody targeting HER2 and PD-L1 inhibits tumor growth with superior efficacy. J. Biol. Chem. *297*, 101420. https://doi.org/10.1016/j.jbc.2021.101420.

19. Cui, J., He, Y., Zhu, F., Gong, W., Zuo, R., Wang, Y., Luo, Y., Chen, L., Wang, C., Huo, G., et al. (2023). Inetetamab, a novel anti-HER2 monoclonal antibody, exhibits potent synergistic anticancer effects with cisplatin by inducing pyroptosis in lung adenocarcinoma. Int. J. Biol. Sci. *19*, 4061–4081. https://doi.org/10.7150/ijbs.82980.

20. Chaganty, B.K.R., Qiu, S., Gest, A., Lu, Y., Ivan, C., Calin, G.A., Weiner, L.M., and Fan, Z. (2018). Trastuzumab upregulates PD-L1 as a potential mechanism of trastuzumab resistance through engagement of immune effector cells and stimulation of IFNγ secretion. Cancer Lett. *430*, 47–56. https://doi.org/10.1016/j.canlet.2018.05.009.

21. Cloven, N.G., Kyshtoobayeva, A., Burger, R.A., Yu, I.R., and Fruehauf, J.P. (2004). In vitro chemoresistance and biomarker profiles are unique for histologic subtypes of epithelial ovarian cancer. Gynecol. Oncol. *92*, 160–166. https://doi.org/10.1016/j.ygyno.2003.09.030.

22. Moasser, M.M. (2007). The oncogene HER2: its signaling and transforming functions and its role in human cancer pathogenesis. Oncogene *26*, 6469–6487. https://doi.org/10.1038/sj.onc.1210477.

23. Slamon, D.J., Clark, G.M., Wong, S.G., Levin, W.J., Ullrich, A., and McGuire, W.L. (1987). Human breast cancer: correlation of relapse and survival with amplification of the HER-2/neu oncogene. Science *235*, 177–182. https://doi.org/10.1126/science.3798106.

24. Buza, N. (2021). HER2 Testing and Reporting in Endometrial Serous Carcinoma: Practical Recommendations for HER2 Immunohistochemistry and Fluorescent In Situ Hybridization: Proceedings of the ISGyP Companion Society Session at the 2020 USCAP Annual Meeting. Int. J. Gynecol. Pathol. *40*, 17–23. https://doi.org/10.1097/PGP.0000000000000711.

25. Valabrega, G., Montemurro, F., and Aglietta, M. (2007). Trastuzumab: mechanism of action, resistance and future perspectives in HER2-overexpressing breast cancer. Ann. Oncol. *18*, 977–984. https://doi.org/10.1093/annonc/mdl475.

26. Fujimura, M., Katsumata, N., Tsuda, H., Uchi, N., Miyazaki, S., Hidaka, T., Sakai, M., and Saito, S. (2002). HER2 is frequently over-expressed in ovarian clear cell adenocarcinoma: possible novel treatment modality using recombinant monoclonal antibody against HER2, trastuzumab. Jpn. J. Cancer Res. *93*, 1250–1257. https://doi.org/10.1111/j.1349-7006.2002.tb01231.x.

27. Fehrenbacher, L., Cecchini, R.S., Geyer, C.E., Rastogi, P., Costantino, J.P., Atkins, J.N., Crown, J.P., Polikoff, J., Boileau, J.-F., Provencher, L., et al. (2020). NSABP B-47/NRG Oncology Phase III Randomized Trial Comparing Adjuvant Chemotherapy With or Without Trastuzumab in High-Risk Invasive Breast Cancer Negative for HER2 by FISH and With IHC 1+ or 2. J. Clin. Oncol. *38*, 444–453. https://doi.org/10.1200/JCO.19.01455.

28. Perez, E.A., Romond, E.H., Suman, V.J., Jeong, J.-H., Sledge, G., Geyer, C.E., Martino, S., Rastogi, P., Gralow, J., Swain, S.M., et al. (2014). Trastuzumab plus adjuvant chemotherapy for human epidermal growth factor receptor 2-positive breast cancer: planned joint analysis of overall survival from NSABP B-31 and NCCTG N9831. J. Clin. Oncol. *32*, 3744–3752. https://doi.org/10.1200/JCO.2014.55.5730.

29. Gianni, L., Lladó, A., Bianchi, G., Cortes, J., Kellokumpu-Lehtinen, P.-L., Cameron, D.A., Miles, D., Salvagni, S., Wardley, A., Goeminne, J.-C., et al. (2010). Open-label, phase II, multicenter, randomized study of the efficacy and safety of two dose levels of Pertuzumab, a human epidermal growth factor receptor 2 dimerization inhibitor, in patients with human epidermal growth factor receptor 2-negative metastatic breast cancer. J. Clin. Oncol. *28*, 1131–1137. https://doi.org/10.1200/JCO.2009.24.1661.

30. Nicolò, E., Tarantino, P., and Curigliano, G. (2023). Biology and Treatment of HER2-Low Breast Cancer. Hematol. Oncol. Clin. N. Am. *37*, 117–132. https://doi.org/10.1016/j.hoc.2022.08.013.

31. Baselga, J. (2010). Treatment of HER2-overexpressing breast cancer. Ann. Oncol. *21*. vii36-40. https://doi.org/10.1093/annonc/mdq421.

32. Su, S., Zhao, J., Xing, Y., Zhang, X., Liu, J., Ouyang, Q., Chen, J., Su, F., Liu, Q., and Song, E. (2018). Immune Checkpoint Inhibition Overcomes ADCP-Induced Immunosuppression by Macrophages. Cell *175*, 442–457.e23. https://doi.org/10.1016/j.cell.2018.09.007.

33. Chakrabarti, J., Koh, V., Steele, N., Hawkins, J., Ito, Y., Merchant, J.L., Wang, J., Helmrath, M.A., Ahmad, S.A., So, J.B.Y., et al. (2021). Disruption of Her2-Induced PD-L1 Inhibits Tumor Cell Immune Evasion in Patient-Derived Gastric Cancer Organoids. Cancers *13*, 6158. https://doi.org/10.3390/cancers13246158.

34. Guven, D.C., Sahin, T.K., Erul, E., Rizzo, A., Ricci, A.D., Aksoy, S., and Yalcin, S. (2022). The association between albumin levels and survival in patients treated with immune checkpoint inhibitors: A systematic review and meta-analysis. Front. Mol. Biosci. *9*, 1039121. https://doi.org/10.3389/fmolb.2022.1039121.

35. Janjigian, Y.Y., Kawazoe, A., Yañez, P., Li, N., Lonardi, S., Kolesnik, O., Barajas, O., Bai, Y., Shen, L., Tang, Y., et al. (2021). The KEYNOTE-811 trial of dual PD-1 and HER2 blockade in HER2-positive gastric cancer. Nature *600*, 727–730. https://doi.org/10.1038/s41586-021-04161-3.

36. Rizzo, A., Mollica, V., Tateo, V., Tassinari, E., Marchetti, A., Rosellini, M., De Luca, R., Santoni, M., and Massari, F. (2023). Hypertransaminasemia in cancer patients receiving immunotherapy and immune-based combinations: the MOUSEION-05 study. Cancer Immunol. Immunother. *72*, 1381–1394. https://doi.org/10.1007/s00262-023-03366-x.

37. Santosa, E.K., and Sun, J.C. (2023). Cardinal features of immune memory in innate lymphocytes. Nat. Immunol. *24*, 1803–1812. https://doi.org/10.1038/s41590-023-01607-w.

38. Yenyuwadee, S., Sanchez-Trincado Lopez, J.L., Shah, R., Rosato, P.C., and Boussiotis, V.A. (2022). The evolving role of tissue-resident memory T cells in infections and cancer. Sci. Adv. *8*, eabo5871. https://doi.org/10.1126/sciadv.abo5871.